

Effect of oxygen on sintering plasmachemical powders of nonoxide high-melting compounds

O.N. Kaidash*

Institute for Superhard Materials of the National Academy of Sciences of Ukraine, 2, Avtozavodskaya St., 254074 Kiev, Ukraine

Received 25 February 1999; received in revised form 13 April 1999; accepted 15 June 1999

Abstract

Electron microscope studies and X-ray structural microanalysis have shown that sintering in the temperature range 800–2000°C proceeds in the solid phase. The granular structure of specimens is due to secondary recrystallization. Development of TiC and TiN recrystallization shows common features but also differences. A common feature is that the centers of grain growth in sintering are not initial nanodispersed powder particles but monocrystalline formations based on pore-free aggregates. The formations are due to coalescence in aggregates at $T_{\text{sint}} > 1000^\circ\text{C}$, caused by the activation of diffusional mobility in TiC and TiN. The latter is due to the oxygen dissolution (which is always present in plasmachemically synthesized powders) in TiC and TiN and the development of neutral highly mobile complexes which include ions of Ti and O in combination with Ti vacancies. At the initial stage of TiC and TiN recrystallization pores are always present at the grain boundaries. Differences are found in the initial recrystallization temperature (T_r) and the influence of grain boundary pores on its development. For TiN T_r is about 1300°C , while for TiC it is about 1400°C . In growing TiN grains, the separation of pores from boundaries takes place at $T = 1400^\circ\text{C}$. This causes the anomalous grain growth. At $T \geq 1400^\circ\text{C}$ the grain growth takes its normal development. In the case of TiC, in the whole range of sintering temperature, the boundaries migrate with pores. © 2000 Published by Elsevier Science Ltd and Techna S.r.l. All rights reserved.

Keywords: A. Sintering; Oxygen effect; Plasmachemical powders; Nonoxides

1. Introduction

At present, when developing ceramic materials based on covalent and ion-covalent substances (such as SiC, B₄C, TiN, TiC, Si₃N₄, AlN, etc.), the microstructural approach is used. It is based on the process development for preparing materials having a tailor-made microstructure, which ensures optimum properties. The basis of the process development is the knowledge of structural-and-phase transformations in an initial substance (or in a combination) under various thermodynamic conditions. In this connection the problem of studying different monophase substances (which differ in dispersion or structural condition) under various sintering conditions is of particular interest because this knowledge is the data base for the design and development of new materials.

Considering that fine ceramics are of particular interest and that such ceramics are mainly prepared from initial high-dispersed powders, we have studied the

grain structure evolution in monophase materials being produced from TiC and TiN plasmachemically synthesized powders.

2. Experimental

Titanium carbide and titanium nitride powders have been the subject of the investigation Table 1. The TiC powder was prepared by reaction between titanium and carbon in a low-temperature hydrogen plasma [1]. Titanium carbide has a cubic lattice of the NaCl-type, the lattice constant $a = 0.4327$ nm (the literature value is 0.4318 nm). Nanodispersed TiN powder was prepared by the company “Neomat” (Riga, Latvia) by nitriding Ti powder in a nitrogen plasma [2].

The powders were cold-pressed in metallic dies into pellets 8 mm in diameter and 2–3 mm thick without a binder and 8 mm in diameter and 15 mm high using a solution of 0.5 wt% synthetic rubber in benzene as a binder for cold-pressing. The compaction pressure was 100–200 MPa, the initial porosity of compacts with

* Tel.: +7-044-435-1321; fax: +7-044-435-3291.

E-mail address: alcon@ismanu.kiev.ua (O.N. Kaidash).

Table 1
Properties of nanodispersed TiC and TiN powders

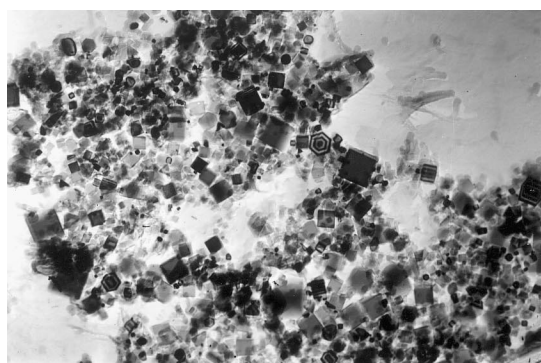
Powder	Specific surface area m ² /g ^a	Average grain size, nm		Contents of element, wt%						Calculational formula of the composition
		EM ^b	X-ray ^c	Ti	C _{total}	C _{free}	N	Impurities ^d		
								O	Cl	
TiC	23	10-80	60	79.00	19.63	0.08	0.05	2.33	0.30	TiC _{0.98}
TiN	58	10-70	35	74.8	—	—	22.3	3.0	—	TiN _{0.90}

^a BET method.

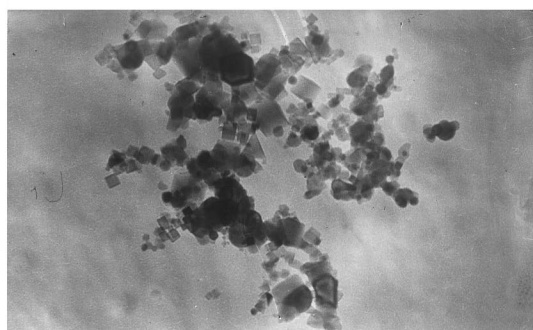
^b By electron microscopy.

^c From the broadening of X-ray diffraction peaks.

^d By neutron-activation analysis.



(a)



(b)

Fig. 1. Micrograph of (a) TiC ($\times 30\,000$) particles and (b) TiN ($\times 40\,000$) particles.

binder 52%, without binder 55%. The specimens were sintered in a furnace with a tungsten heater in a vacuum of 7×10^{-3} Pa or in highly pure nitrogen at 0.03 MPa. To measure shrinkage, a high-temperature dilatometer was used.

Fracture surfaces of the specimen were observed in a SU-10 scanning electron microscope. The surfaces were spray-coated with carbon (a carbon layer no more than 10 nm thick) to prevent them from being charged.

3. Results and discussion

3.1. Nanodispersed TiC and TiN powders

Electron microscope studies have shown that particles of TiC and TiN nanodispersed powders were 10–80 nm in size [3] and had a pronounced monocrystalline form (Fig. 1). The structure has been of the NaCl-type, the majority of the TiC and TiN particles were in the form of cubes made up of six (100) planes. Observed were also tetrahedrons with four (111) planes and rhombododecahedrons with twelve (110) planes. These forms of particles are typical for transition metal nitrides and carbides prepared by plasmachemical synthesis, while particles of CVD Ti and V nitrides of the same size are of the spherical form. As in NaCl-type structures, the

(100) faces have a minimum surface energy, the predominant form of particle growth is based on cubic crystals with (100) planes.

3.2. Sintering of TiC

Fig. 2 shows the relative density of TiC specimens, prepared with a binder (initial density 48%) and without a binder (initial density 45%) as a function of sintering temperature, the isothermal holding time being 1 h.

Figs. 3–5 show the grain size distribution in sintered TiC-specimens processed with a binder in the initial compacts which are based on the evaluation of grain

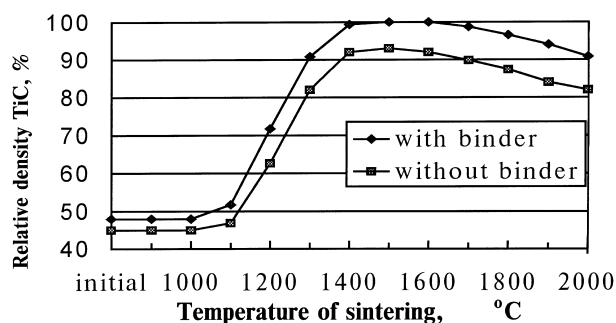


Fig. 2. Densification behavior of TiC vs. sintering temperature (◆, processed with binder and ■, without binder).

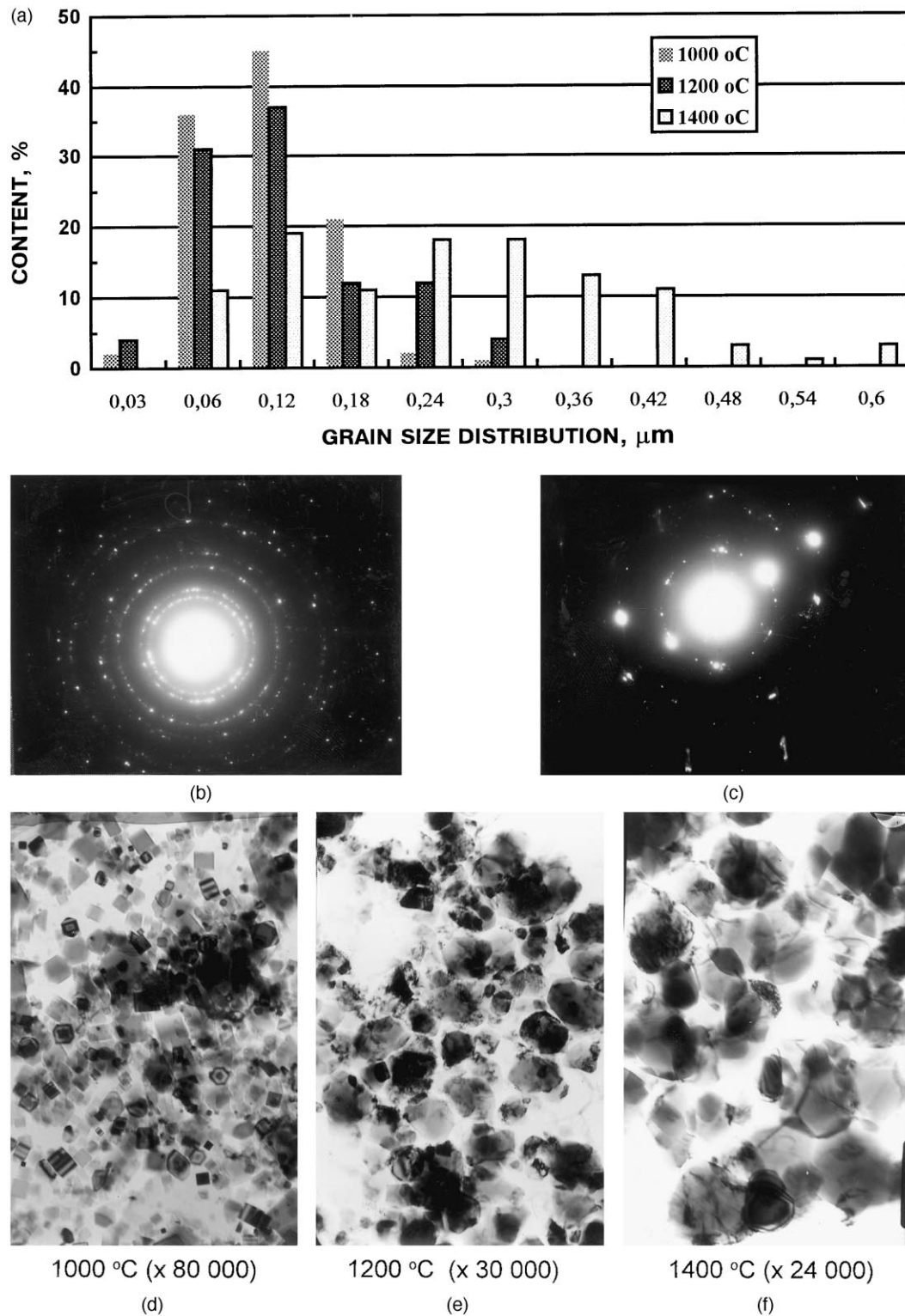


Fig. 3. Histograms of grain-size distribution (based on removed particles) (a), electron micrograph of removed particles (b,c) and characteristic appearance of removed particles (d,e,f) in TiC specimens processed with a binder and sintered at temperatures of: 1000°C (b,d) ($\times 80\,000$); 1200°C (e) ($\times 30\,000$) and 1400°C (c,f) ($\times 24\,000$).

sizes from removed particles and replicas. Also shown are characteristic electron microscopic images of the grain structure and electron micrographs from removed

particles. In Fig. 5d (sintering temperature of 2000°C) an image of a group of grains in a specimen in the form of a fine foil is shown, which was prepared by

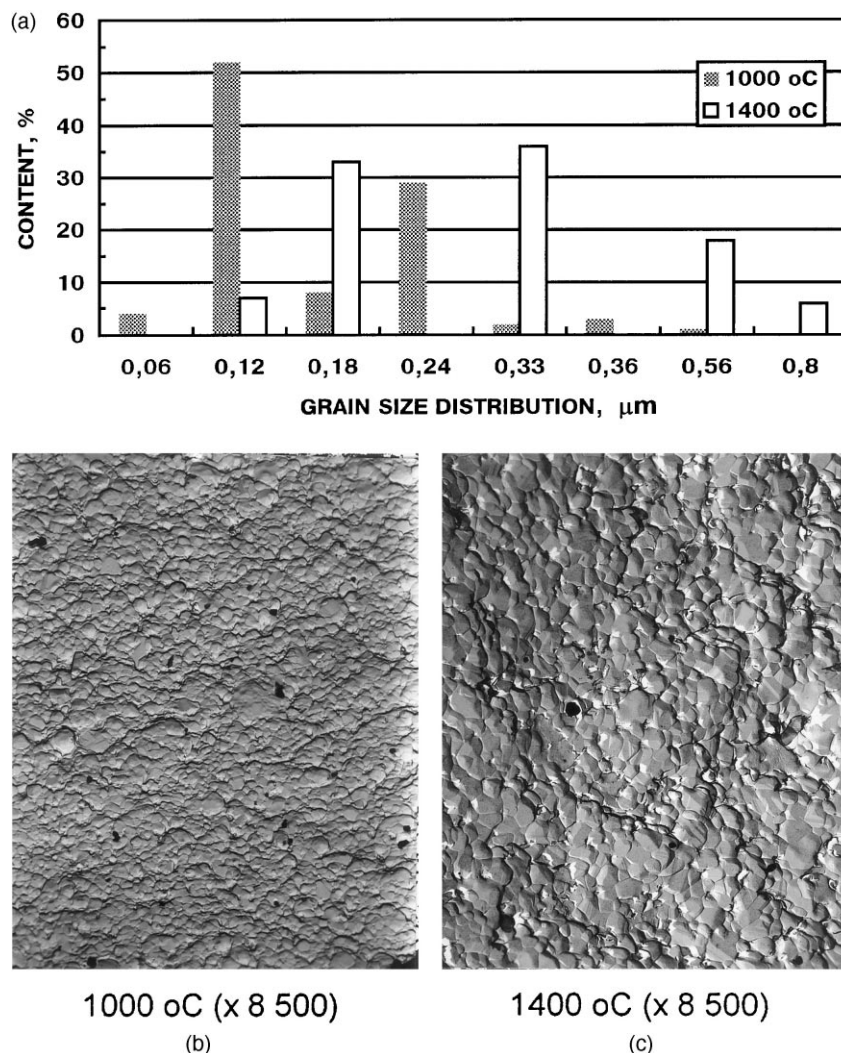


Fig. 4. Histograms of grain-size distribution (based on replicas) (a) and SEM images of grains in TiC specimens processed with a binder and sintered at temperatures of: 1000°C (b) and 1400°C (c) ($\times 8500$).

ion-thinning. The results have been analyzed considering the mechanisms of the microstructural development in specimens with increasing sintering temperature and investigation of the grain structure (from replicas, removed particles and fine foils).

3.3. Grain structure development with increasing sintering temperature

As evident from the above data analysis, the pronounced densification of compacts with a binder begins at 1200°C; at 1400°C they become pore-free. Starting from 1600–1700°C the material density decreases. In specimens without a binder, a pore-free state is not obtained and at temperatures of 1400–1600°C their porosity is 8%.

Comparison of the grain size distribution in specimens and particles in the initial powder has shown that starting from a temperature of 1000°C a slight coarsen-

ing of grains occurs to form pore-free polycrystalline aggregates (Fig. 3d).

Diffraction microanalysis shows that even at 1400°C the aggregates are generally monocrystalline and are equiaxed (Fig. 3f). With a temperature increase to 1600–2000°C, the size of monocrystalline grains increases and at the grain boundaries there appear pores. In most cases the pores are round in form or exhibit a tendency towards a hexagon, which is shown in Fig. 5b–d. The oxygen concentrates at grain boundaries and with an increase in sintering temperature the oxygen content of specimens decreases. No phases at grain boundaries, including oxygen-containing ones, have been revealed by electron microscopy. X-ray studies also show that oxide phases are not present in specimens. This allows a conclusion that oxygen is dissolved in TiC and grain boundary regions are enriched with it.

It is evident from the above data that in the temperature range under study, sintering of a plasmachemical

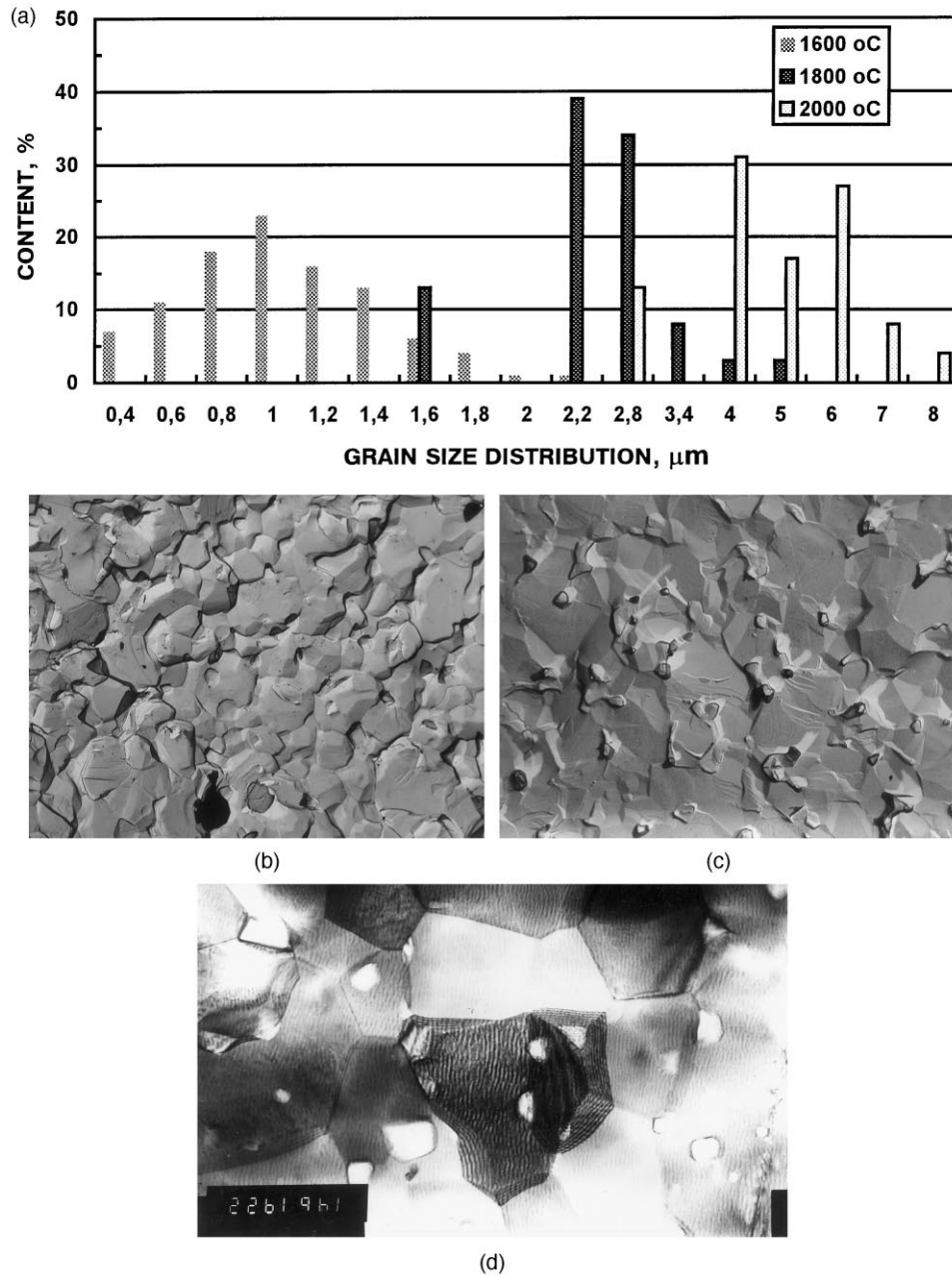


Fig. 5. Histograms of grain-size distribution (based on replicas) (a). SEM images of grains in TiC specimens (b,c) and image of a group of grains (the foil prepared by the ion-thinning method) (d) in TiC specimens processed with a binder and sintered at temperatures of: 1600°C (b) ($\times 9600$), 1800°C (c) ($\times 10\,000$), 2000°C (d) (15 000).

TiC powder proceeds only due to solid-state structural transformations. Coarsening grains due to recrystallization proceeds in the specimens starting from a temperature of 1400°C, i.e. as soon as a highly dense condition is attained. The main feature is that the centers of grain growth are not initial monocrystalline dispersed particles, but monocrystalline formations based on pore-free polycrystalline aggregates. Analysis of the evolution of the structural transformations in the polycrystalline aggregates which proceed in the temperature range 1000–1400°C and are observed in the removed particles

shows that at first there appear aggregates with some contacts and well-defined boundaries between grains, then (at 1200°C) such boundaries become diffuse (wide) and at a temperature of 1400°C they disappear completely. At the same time boundaries form between aggregates (which are now monocrystalline). Judging by the pronounced coarsening of grains at 1400°C such boundaries are highly mobile. At a temperature of 2000°C, as is evident from the grain structure analysis on fine foils, the boundaries are highly angular, well formed, defect-free, but with the presence of pores (Fig. 5d).

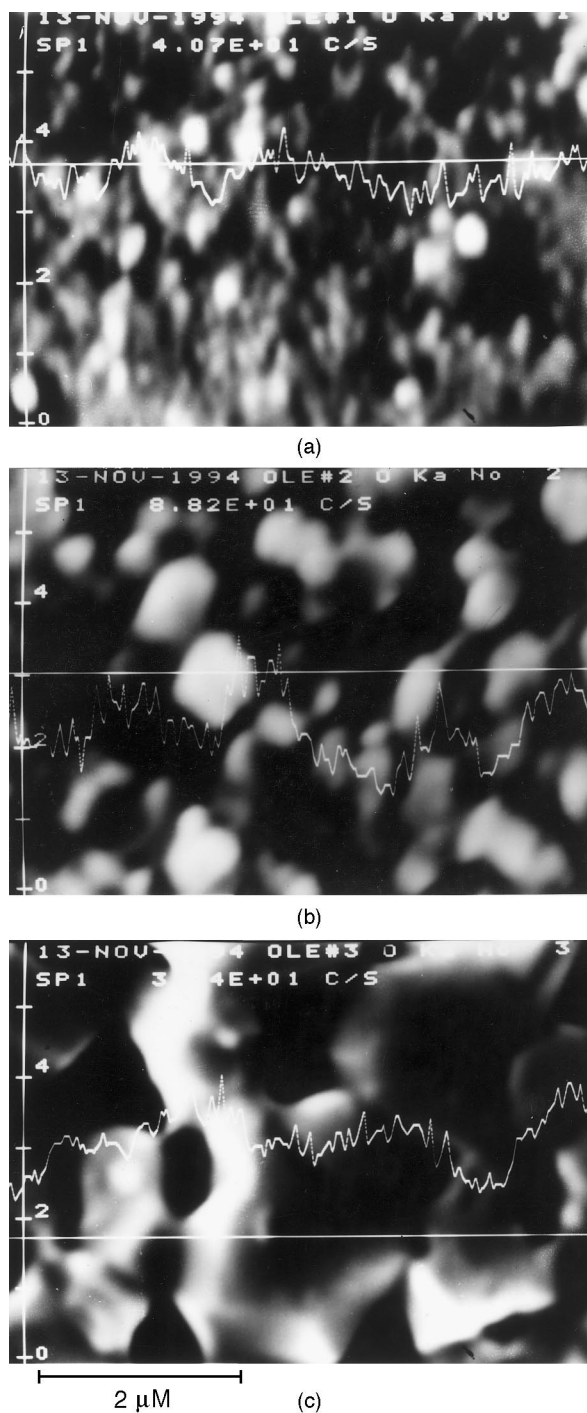
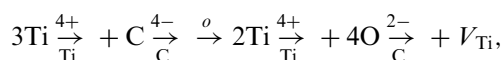


Fig. 6. Oxygen distribution curves for TiC specimens sintered at 1000°C (a), 1400°C (b), 1600°C (c).

The curves of oxygen distribution over the surface of polished TiC specimens demonstrate that the peak height decreases with an increase in sintering temperature and hence, grain size (Fig. 6). The latter confirms the fact that oxygen is localized in near-boundary zones of the grains. The peculiarities of the of grain structure development allow us to assume the following scheme

of successive structure transformations in nanodispersed TiC particles with increasing sintering temperature:

1. The formation of mechanical contacts between powder particles of plasmo-chemical powders, both in loose form and in cold-pressed compacts.
2. The interaction between oxygen adsorbed on the particle surface and titanium carbide to form titanium oxide or oxycarbide followed by the formation of isomorphic three-component substitutional solid solution (oxygen substitute for carbon) in the titanium carbide-titanium oxycarbide system. It is known [5], that oxygen is capable of performing isomorphic substitution for carbon and nitrogen in their compounds with transition metals. This process may be given as:



(V_{Ti} is the vacancy in the titanium sublattice).

3. The Ti vacancies — activated diffusion coalescence of TiC in a polycrystalline aggregate to transform it into a monocrystalline grain. The grain is essentially a solid solution of oxygen in TiC. Oxygen in TiC, using the conception of structure of solid solutions of isomorphic heterovalence substitution [6], presents in the form of complexes of the $2\text{Ti}^{4+} + 4\text{O}^{2-} + V_{\text{Ti}}$ composition.

In parallel with the monocrystallization of polycrystalline aggregates physical contacts are formed, i.e. intergranular boundaries between them — the migration of these boundaries determines the recrystallization coarsening of grains. The development of pores at the grain boundaries and thus the density decrease at temperatures of 1600°C are explained through an analysis of the following fractograms. According to [4] at a temperature of 1500°C there occur the dissociation of the solid solution and the dissociation of TiC_xO_y -oxycarbide to form carbon oxide. The reaction proceeds naturally in TiC-grain boundaries which promotes the formation of gas filled closed pores. As the reaction proceeds, the surface layers become poor in oxygen (due to the appearance of a concentration gradient oxygen migration takes place in the near-boundary regions and the reaction proceeds further. Pores formed at temperatures of 1500–1600°C coalesce at higher temperature and are trapped at the migrating boundaries. The pores are coarsened due to the coalescence of smaller pores which result from the proceeding gas-forming reaction at the boundaries (Fig. 5d).

An analysis of the histograms shown in Figs. 3–5 suggests that for all variety of specimens under study there is no agreement between the maxima when results from replicas and removed particles are compared. In the case of the analysis by replicas the distribution maximum shifts

to higher values. The microstructural analysis of removed particles shows that this fact can be explained by peculiarities of the sintering of nanodispersed TiC powders. The initial stage of sintering these powders proceeds due to the formation of dense aggregates consisting of several initial grains. Subsequently the aggregates become monocrystalline and centers of new grains (recrystallization centers). This is evident from a comparison of the initial grain morphology (Fig. 1) and their images in removed particles of specimens prepared at 1000, 1200 and 1400°C (Fig. 3). Analysis of the removed particles reveals well defined boundaries of individual grains which can be aggregated. Therefore, the grain size defined by removed particles, correspond to the real grain size distribution in a specimen. If the grain size analysis is based on a replica, the reference points are the boundaries along which the intercrystalline fracture occurs (Figs. 4 and 5). Specimens, which form aggregates in sintering, fail usually along the interfaces of aggregates. For this reason, the fracture planes of specimens (and thus replicas from such fractures) show no single grains but groups of them which

make up the aggregates. The fact that a great number of grains form aggregates (especially at sintering temperatures of 1300–1400°C) is responsible for the larger grain size values as obtained with replicas.

SEM observations of fractured specimen show that the identification of grain boundaries is possible only in specimens sintered at temperatures above 1400°C. The comparison of fractograms of samples after sintering at 1400 and 1600°C, gives conclusive evidence of this fact. Thus, in specimens sintered at 1000–1400°C the grain size should be evaluated in removed particles only. For specimens sintered at higher temperatures the use of electron microscopy (replica) and SEM (natural fracture) is possible. In the latter case, a grain should be larger than 1 µm.

3.4. The influence of a binder on sintering nanodispersed TiC powders

It was shown above that the presence of a binder results in the highest specimen density at a temperature

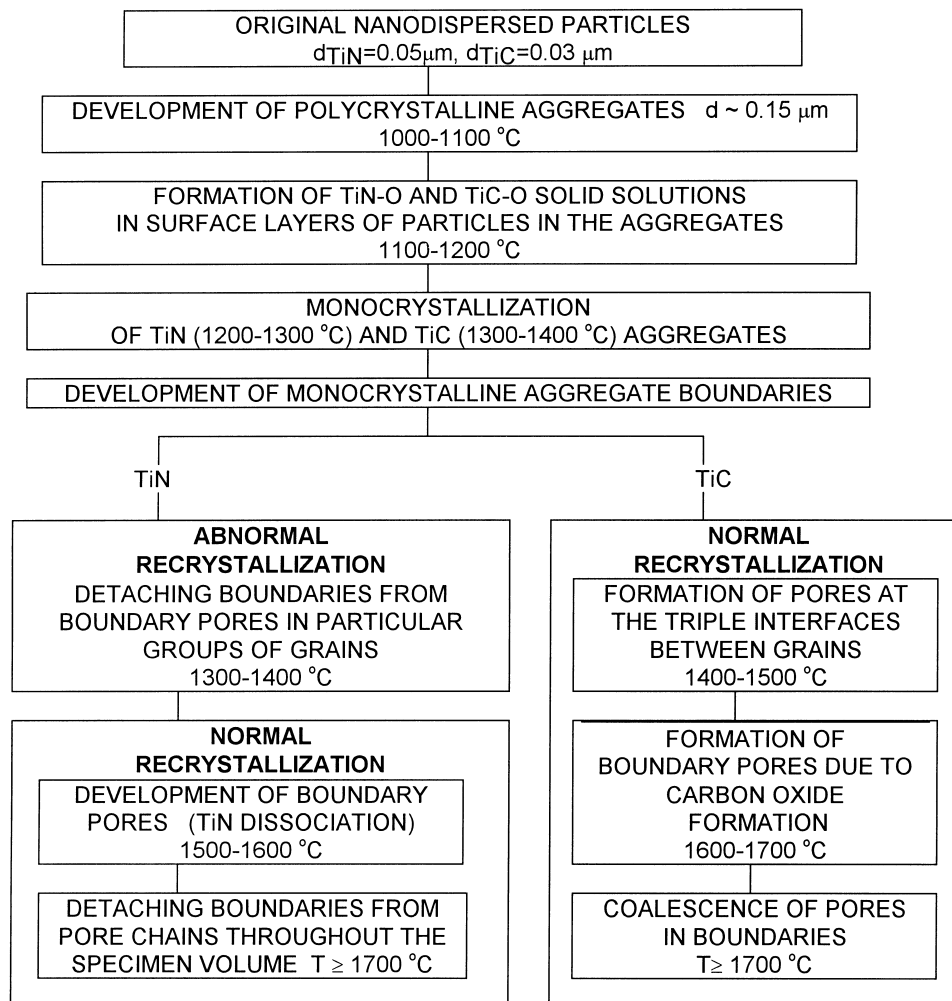


Fig. 7. Schematic representation of the grain structure development in sintering TiN and TiC nanodispersed powders.

Table 2

Estimation of the driving force of recrystallization (ΔG) and the opposing force (F) created by pores in sintering TiC (processed with binder)

T_{sint} (°C)	1600	1800	2000
$\Delta G \times 10^{-7}$ J/m ³	12.5	5.6	2.3
$F \times 10^{-7}$ J/m ³	5.4	2.4	2.3

of 1400°C; in a case of binder-free sintering at 1400 and 1600°C, the sample porosity is 8%. In this case, at 1600°C the grain size of the latter specimens are somewhat coarser. This fact may be explained by the more intensive proceeding of a pore-formation reaction at the boundaries (due to an increase of carbon content) and thus, by a higher concentration of pores at the boundaries, which retard the migration. The latter stems from the following consideration. In Table 2 the driving force of recrystallization ΔG and an opposing force F created by pores for specimens sintered in the temperature range 1000–2000°C is estimated. ΔG for recrystallization has been estimated from $\Delta G = 2\gamma_g/R$, where γ_g is the free boundary energy taken to be 0.5 J/m², R is the TiC grain size.

The opposing force is estimated from $F = fF_d/(\gamma r^2)$, where f is a part of area occupied by internal defects of spherical form per 1 cm² of material surface ($f = 0.05$).

The opposing force created by a defect, F_d , is given by $F_d = \pi r \gamma_g$, where r is the defect size, γ_g is the free energy at the interface (taken to be 0.5 J/m³).

The condition of migration of boundaries with pores is $\Delta G > F$. The above data show that for all three cases $\Delta G > F$, i.e. the conditions of migration of boundaries with pores are realized.

A schematic representation of the of grain structure development during sintering nanodispersed TiC and TiN powders based on the concepts discussed above is given in Fig. 7.

4. Sintering of TiN

Fig. 8. shows the relative density of sintered TiN specimens processed with a binder as a function of temperature after sintering in nitrogen and in vacuum, holding time being 1 h.

The TiN powder morphology is shown in Fig. 1. Histograms of the grain size distribution in specimens sintered at 1200–1700°C in vacuum are given in Figs. 9 and 10.

In a qualitative sense, the microstructural changes in the TiN specimens proceed like those in the TiC specimen. The formation of polycrystalline aggregates of TiN particles, their monocrystallization, the development of grain boundaries between them, and the subsequent new grain growth proceed similarly to those for TiC. At the

same time difference is observed in the grain growth development between TiN and TiC specimens. First, TiN specimens show an appreciable grain growth even at a sintering temperature of 1300°C, while TiC specimens at a temperature of 1400°C. At this temperature in TiN large grains develop with circle of pores inside them. In specimens sintered in nitrogen such grains are rarely found, in those sintered in vacuum they occur more often. The histograms of the grain size distribution in TiN specimens (Fig. 9) show a second peak. This points to the occurrence of an anomalous grain growth.

The development of the grain structure in TiN specimens at a sintering temperature of 1400°C has a number of peculiarities depending on the sintering atmosphere. During vacuum sintering at 1500°C pore formation is observed at grain boundaries; at higher temperatures ($T > 1700^\circ\text{C}$) the pore concentration increases (their mean size increases) and the distance between them decreases — they are observed in near-boundary zones of the grains (Fig. 10), pore-free boundaries migrate. This situation is also observed in specimens sintered in nitrogen. But, the detachment of boundaries from the lines of pores is practically observed in the whole specimen volume even at 1600°C.

The above data on the microstructural transformations in TiN specimens during sintering show that at temperature of 1300°C anomalous recrystallization occurs, which is caused by the pore detachment from the boundaries. A recrystallization of this kind was formerly observed in sintering studies of submicron powders of ZrO₂, Al₂O₃, BaTiO₃ etc. [7–9] At temperatures between 1400 to 1600°C and higher a uniform grain structure is formed (Figs. 9 and 10), which is indicative of normal secondary recrystallization. The presence of lines of pores within the grains points to their growth due to the migration of a boundary, which was detached from pores in an earlier stage.

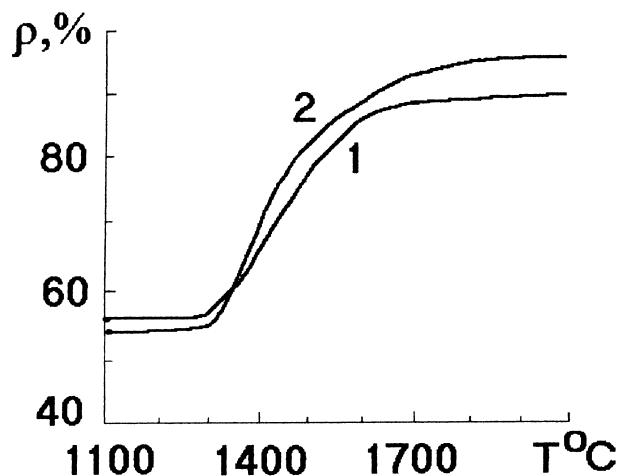


Fig. 8. Densification behavior of TiN vs. sintering temperature (1, in vacuum, 2, in nitrogen).

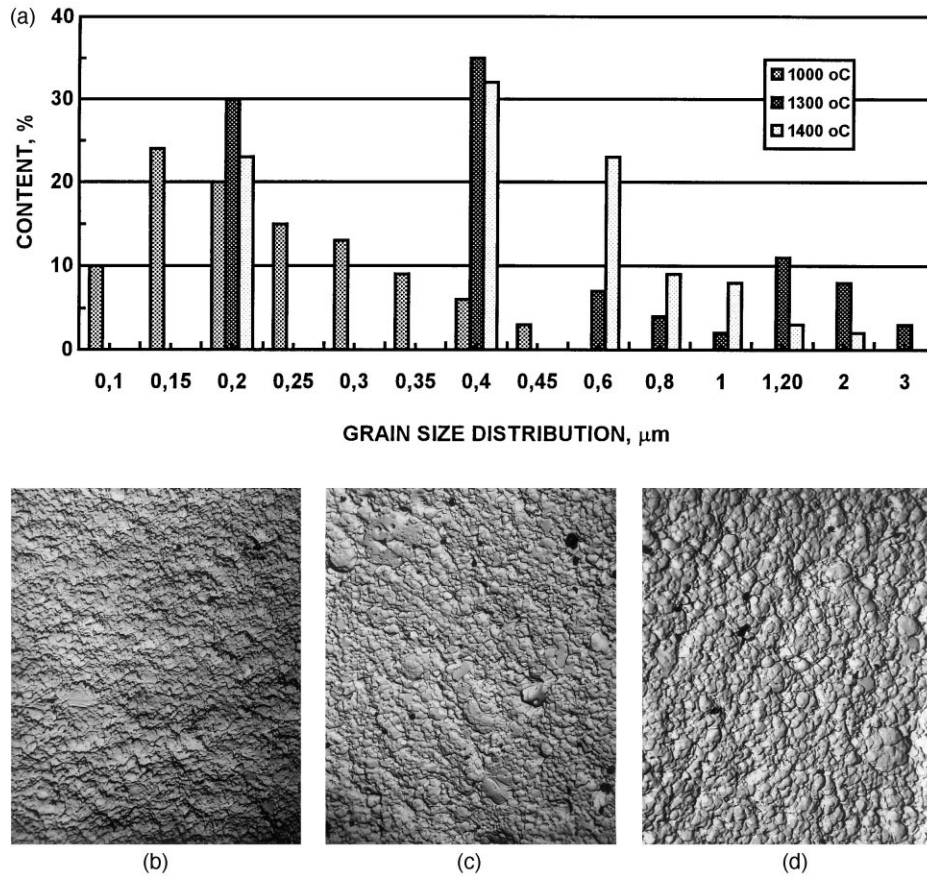


Fig. 9. Histograms of grain-size distribution (from replicas) (a) and SEM images of grains in TiN specimens sintered in vacuum at temperatures of: 1000°C (b), 1300°C (c) and 1400°C (d) ($\times 8500$).

An estimation of the driving force for the secondary recrystallization in TiN at various temperatures (based on the mean grain size) and a opposing force due to the presence of pores are shown in Table 3. It is evident from the results that at sintering temperature of 1700°C the driving force of the recrystallization considerably exceeds the opposing force.

The driving force of the secondary recrystallization decreases with an increase in the sintering temperature. The opposing force estimated from r of pores enclosed in grains far exceeds the driving force of recrystallization. A distinct grain growth at temperatures above 1600°C allows the conclusion pores become detached from the boundaries just at $T = 1600^\circ\text{C}$.

Table 3
Results of estimation of the driving force of recrystallization (ΔG) and pore-caused opposing force (F) in sintering TiN

Medium	Vacuum		Nitrogen	
T_{sint} ($^\circ\text{C}$)	1300	1700	1400	1700
$\Delta G \times 10^{-7}$, J/m ³	7.0	2.0	4.1	2.2
$F \times 10^{-7}$, J/m ³	25.0	4.2	8.0	3.0

As shown in Fig. 8, the change in density of TiN specimens sintered in various media increases with temperature but does not reach 100%. The development of pores in boundaries at temperature of 1500–1600°C, i.e. at a high-density state ($\sim 94\%$) may be associated with a change in the stoichiometry of TiN, i.e. a depletion in nitrogen. The resulting development of vacancies activates the sample densification, on one hand, and promotes the appearance of micropores in boundaries on the other. The latter retards the grain migration and thus, grain growth. This peculiarity of the TiN structural development and its influence on the density and microstructure of specimens as a whole explain the more significant coarsening of grains in specimens sintered in nitrogen as compared with those sintered in vacuum at a temperature of 1700°C. In a nitrogen atmosphere, the depletion of TiN in nitrogen is less intensive than in vacuum, the development of pores in boundaries is less intensive and, consequently, the opposing force is low (Table 3). The detachment of boundaries from pores in this case occurs at a lower driving force of recrystallization. As evident from the above data, for all the cases F exceeds ΔG , that confirms the experimental observation that boundaries are detached from pores.

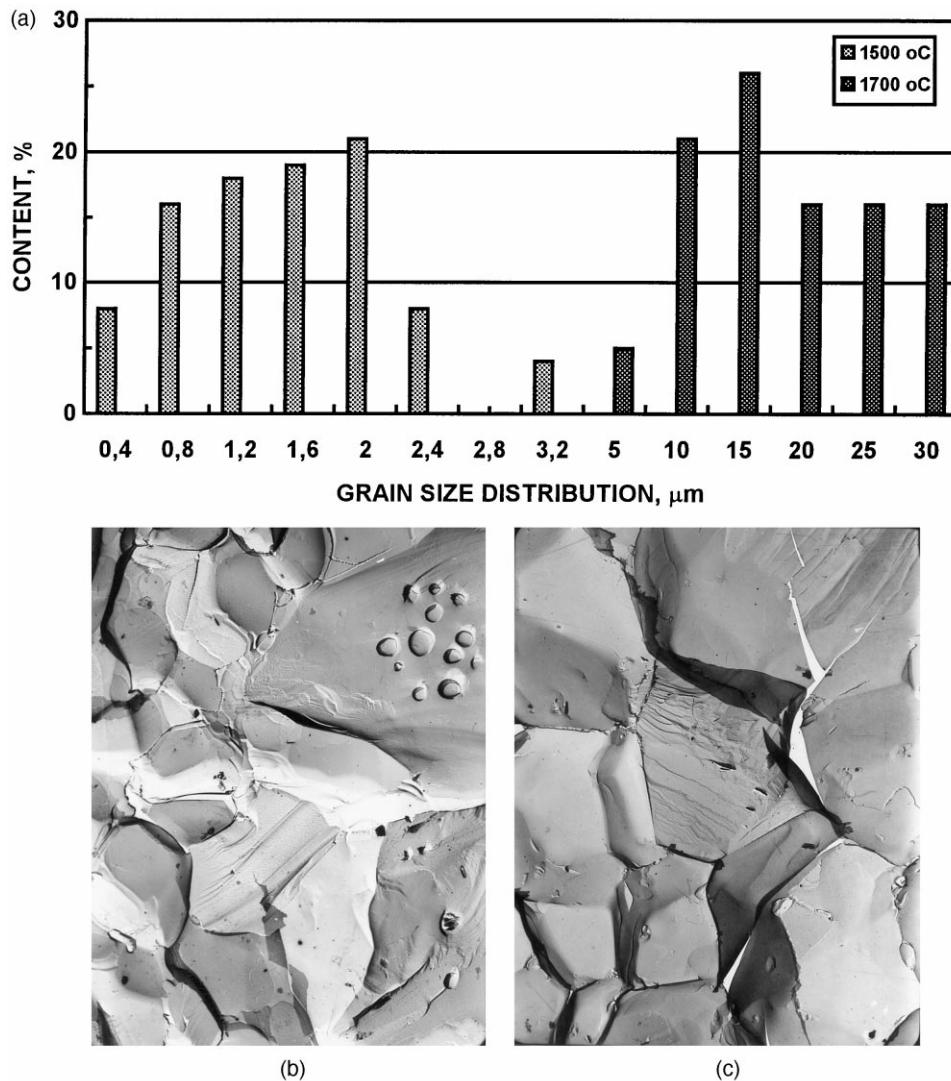


Fig. 10. Histograms of grain-size distribution (from replicas) (a) and SEM images of grains in TiN specimens sintered in vacuum at temperatures of: 1500 °C (b) and 1700 °C (c) ($\times 7500$).

5. Conclusions

1. The microstructure of polycrystalline specimens prepared from TiC and TiN powders (mean size of TiC particles 30 nm, mean size of TiN particles 50 nm) was studied by electron microscopy: of carbon replicas from fracture surfaces, from removed particles, derived on replicas of such fractures, and by scanning electron microscopy of fractured surfaces.

It has been found that in specimens sintered at $T_{\text{sint}} = 1000\text{--}1400^\circ\text{C}$ the grain size should be determined only in removed particles. For specimens sintered at higher temperatures, electron microscopy of replicas and SEM of fractured surfaces may be used. In the latter case the grain size in specimens should be more than 1 μm .

2. It has been found that sintering proceeds in the solid phase. The microstructure in specimens develops by a secondary recrystallization mechanism. Common features and differences have been revealed in the microstructural development of TiC and TiN specimens. In both cases the centers of grain growth in sintering are not initial nano-dispersed particles but monocrystalline formations based on pore-free aggregates. Such formations develop due to chemicoalescence in the aggregates at $T_{\text{sint}} = 1000^\circ\text{C}$, caused by the activation of TiC and TiN diffusion ional mobility. The latter is supposed to be due to the dissolution of oxygen (which is always present in plasmachemically synthesized powders) and the development of neutral highly mobile complexes which include ions of Ti and oxygen in combination with vacancies of Ti.

At the initial stage of TiC and TiN recrystallization there are pores at the grain boundaries. Differences are found in the initial temperature of secondary recrystallization (T_r) and in the influence of grain boundary pores on its development. For TiN $T_r = 1300^\circ\text{C}$ and for TiC $T_r = 1400^\circ\text{C}$. This causes the development of anomalous grain growth. At $T \geq 1400^\circ\text{C}$ the grain growth takes its normal coarse stage. In the case of TiC in the sintering temperature range under consideration the boundaries migrate with pores.

3. The development of anomalous recrystallization in TiN specimens at $T_{\text{sint}} = 1300\text{--}1400^\circ\text{C}$ has been established. The recrystallization is shown to be due to the detachment of a boundary from a line of boundary pores. The driving force for the secondary recrystallization in TiN and TiC and the opposing force due to pores have been calculated. In the case of TiN in the temperature range $1300\text{--}1400^\circ\text{C}$ the latter prevails. Just this fact is responsible for the development of the anomalous recrystallization. As far as TiC is concerned, the motive force always exceeds the opposing force. Just this fact is responsible for the migration of boundaries with pores.
4. It is shown that the pore formation in sintering TiC specimens at T_{sint} above 1500°C can be explained by the reaction of gas formation in boundaries caused by the decomposition of TiC_xO_y . The pores which are formed at temperatures of $1500\text{--}1600^\circ\text{C}$, are attached to migrating bound-

aries at higher temperatures. Along with this observation the coarsening of pores by coalescence with smaller pores takes place, which develop due the proceeding gas-forming reaction at the boundaries. This process decreases the oxygen content of the material with increasing sintering temperature.

References

- [1] J.P. Grabis, G.N. Miller, M.N. Heidemane, Formation of transition metal nitrides in high-temperature nitrogen's stream/ Papers II Symposium on plasmachemistry, Riga, Zinatne (1975) 164–167.
- [2] A.M. Lykov, Yu.N. Mamontov, A.L. Surzh, et al., Investigation of dispersivity plasmachemical titanium carbide, Papers Plasma-chemistry-79, Science, Moscow (1979) 35–39.
- [3] M.I. Mendelson, Average grain size in polycrystalline ceramics, *J. Am. Ceram. Soc.* 52 (8) (1969) 443–446.
- [4] S.I. Alyamovskiy, Yu.V. Zanuulin, G.P. Shveikin, Oxidicarbides and oxinitrides of IVA and VA subgroups' metals. Moscow, Science (1981) 144.
- [5] E.S. Makarov, Isomorphism of atoms in crystals. Moscow, Atomizdat (1978) 286.
- [6] V.S. Urusov, Theory of isomorphous mixing. Moscow, Science (1977) 251.
- [7] G.S. Oleinik, M.A. Kuzenkova, O.A. Shevchenko, Mechanism of formation self-reinforced AlN-materials–Elektronnaya microscopy and strength of materials, IPM NAS Ukraine (1994) 78–94.
- [8] M.X. Shoshorov, V.I. Alymov, Ultradispersed and amorphous materials in powder metallurgy technology, *Mater. Sci.* 1 (1997) 51–54.
- [9] Ya.E. Geguzin, V.I. Kibets, Diffusion creep of polycrystals with intergrain phase layer, *Physics of Metal and Material Science* 36 (5) (1997) 1043–1050.